THE ASTROPHYSICAL JOURNAL, 236:628–644, 1980 March 1

OPTICAL EMISSION FROM SHOCKS. VI. ABUNDANCE GRADIENT IN M33 FROM SUPERNOVA REMNANTS

MICHAEL A. DOPITA[1]
Mount Stromlo and Siding Spring Observatories, Research School of Physical Sciences, Australian National University

AND

SANDRO D'ODORICO AND PIERO BENVENUTI[2]
Osservatorio Astronomico di Asiago, Università di Padova
Received 1979 April 9; accepted 1979 September 13

ABSTRACT

The absolute abundance gradient in the spiral arms of the galaxy M33 has been obtained using supernova remnants (SNRs) as a tracer of gaseous phase abundance in the interstellar medium. No galactic enrichment theory is entirely successful in explaining the observations. The gradient in N/S abundance obtained from SNRs is identical to that given by H II region observations. Nitrogen seems to be produced first as a primary but later (at higher enrichment and star mass to gas mass ratio) as a secondary nucleosynthesis element.

Subject headings: galaxies: individual — nebulae: abundances — nebulae: supernova remnants

I. INTRODUCTION

Aller (1942) was perhaps the first to notice a systematic variation in line intensity ratios of H II regions in external galaxies with their projected distance from the galactic center. Searle (1971) realized that this could be due to large-scale abundance gradients in the interstellar medium, and in a pioneering study of six Sc galaxies attempted to quantify this effect. Since then there have been many further studies, notably by Benvenuti, D'Odorico, and Peimbert (1973), Comte (1975), Smith (1975), Jensen, Strom, and Strom (1976), Sarazin (1976), Collin-Souffrin and Joly (1976), Shield and Searle (1978), and Hawley (1978), all of whom observed spiral galaxies. Our own Galaxy has been observed principally by Sivan (1976) and Peimbert, Torres-Peimbert, and Rayo (1977), and an abundance gradient was found. The H II regions in the Magellanic Clouds have been looked at by Peimbert and Torres-Peimbert (1974), Dufour (1975), Dufour and Harlow (1977), and Pagel *et al.* (1978) (with the results in these systems that the abundance gradient, if it exists, is very small).

In general, studies following that of Searle (1971) have been marked by an increasing respect for the difficulties of interpretation of the line ratio gradients. Some of the factors which may be important are as follows:

1. Any helium abundance gradient will produce a gradient in the photoionizing spectrum of the existing stars and hence an excitation gradient in the H II region.

2. Abundance gradients may produce variations in the initial mass function of heavy stars and hence excitation gradients.

3. Local gas density and other factors such as strength of the spiral shock may produce similar effects.

4. The presence of dust (the density of which is governed by a whole host of formation and destruction which are themselves strong functions of the galactocentric distance) can either directly alter gaseous phase abundances or, by absorption, alter both the temperature and ionization structure of the H II regions (Petrosian 1973; Mezger, Smith, and Churchwell 1974; Dopita 1974).

5. Clumping of the gas tends to enhance lines of low excitation [O II], [S II], [O I], etc.). This occurs either as a result of higher densities close to the ionization front or by shadowing of the direct radiation field from the star by dense neutral globules (Van Blerkom and Arny 1972).

6. Because of the difficulty of measuring temperatures of either the high-ionization (O^{++}, N^{++}, He^{+}, H^{+}) or the low-ionization (O^{+}, N^{+}, He^{0}, H^{+}) zones of the H II regions (which together account for the bulk of the ionized gas), few absolute abundances have been derived. The importance of temperature fluctuations or systematic differences in temperature between the two zones (expected on theoretical grounds) remains a matter of guesswork.

The fact that this depressing catalog of problems has not deterred investigators in the field is perhaps a testament to the importance of the central problem. For, if accurate gas phase abundances can be derived, we will have a Rosetta stone which will enable us at once both to discover the sources of chemical enrichment of the gas and to unravel the past dynamical evolution of spiral galaxies.

[1] Guest Investigator, Hale Observatories, 1978.

[2] At present at ESA Villafranca satellite tracking station, Madrid, Spain.

A possible way of sidestepping some of the above problems is to find a tracer, other than the H II regions, of gas phase abundances in the interstellar medium. Such a tracer appears to be found in the supernova remnants (SNRs).

Perhaps the first reasonably accurate attempt to model the spectrum of a supernova to give both shock conditions and elemental abundances in the shocked interstellar material was by Cox (1972*a*, *b*). Since then, earlier papers in this series have addressed themselves to this problem. In Paper I (Dopita 1976) a specific model was applied to observations by Osterbrock and Dufour (1973) of Large Magellanic Cloud (LMC) supernova remnant, N49. This study showed a general underabundance of O, S, Ne, and in particular N compared with the Sun—a result in broad agreement with the H II region observations (Peimbert and Torres-Peimbert 1974; Dufour 1975; Pagel *et al.* 1978). Paper II (Dopita 1977*a*) investigated the effects of shock conditions and abundances and gave an interpretive set of diagnostic diagrams, which were used in Paper III (Dopita, Mathewson, and Ford 1977) to give abundances of many SNRs in the Galaxy and the Magellanic Clouds. Despite a large scatter, due principally to limitations of the spectroscopic data and (to a lesser extent) limitations in the modeling, a clear ordering of chemical enrichment from the SMC through the LMC to our Galaxy was found. Nitrogen appeared to be mainly a secondary nucleosynthesis element, that is to say, an element formed in second generation stars from elements produced by the first generation.

Possible errors in the modeling procedure are much easier to quantify following publication of the sophisticated models of Raymond (1976, 1979) and Shull and McKee (1979) (the latter authors have been able to build self-consistent models for the preionization problem discussed in Papers I and II). The extent to which these errors are important and to which the observed abundances in SNRs can be thought as representative of normal interstellar gas are discussed in § IV.

The identification of SNRs in external spiral galaxies is in its infancy. Rubin, Kumar, and Ford (1972) found seven nebulosities having the characteristic spectrum of a shocked gas in M31. These were subsequently discussed in more detail by Kumar (1976). In M33 five candidates were selected from interference photography by D'Odorico, Benvenuti, and Sabbadin (1978), of which two appear as distinct sources on the 21 cm continuum map by Israel and van der Kruit (1974). Although such a detection does not confirm a SNR identification before a measurement of a spectral index, it does make it more probable. These two radio-emitting objects and one other candidate were spectroscopically confirmed as SNRs (Danziger *et al.* 1979), and an attempt was made to estimate abundances.

During the last year, a complete survey for SNRs in M31, M33, NGC 45, 55, 256, 300, 2403, 4449, 6822, and IC 342 has been completed using the Schmidt telescopes at Siding Spring and Hale Observatories and the 1.8 m reflector at Asiago, the results of which are to be published as a catalog (D'Odorico, Dopita, and Benvenuti 1979*a*). In each of both M33 and M31 some 19 candidates have been isolated, and this paper reports spectroscopic observations with the 5 m Hale telescope of 12 of these at various radial distances from the center of M33. Seven bright H II regions which occur close to these SNRs have also been observed in order to compare abundance trends, and we also present new spectrophotometry of two SNRs in the Galaxy, two in the LMC, and one candidate in M31.

II. OBSERVATIONS AND THEIR REDUCTION

The observations of M33 and M31 were made during the nights of 1978 September 9–11 with the SIT spectrograph (Gunn *et al.* 1979) at the Cassegrain focus of the 5 m Hale telescope. This was used with a 500 line mm^{-1} grating which gave a spectral coverage from 3600 to 6900 Å at a resolution of 12 Å. The entrance slit subtended $2'' \times 61''$ in the focal plane, extended in the E–W direction. Allowing for guiding errors on the objects, many of which were invisible in the guide TV, the effective spatial resolution of the data along the slit was about 2″, so that very good separation of the SNR spectrum from possible contamination by H II regions was achieved.

Integration times on the SNR varied between 300 and 2700 s, but went as low as 50 s for the H II regions. Flat-field calibrations were made using a diffuse white light source, and calibration of the spectral sensitivity was made by observing Oke (1974) white dwarf standards.

Reduction to relative intensities was made using the range of panoramic and spectral data programs available on the HP2100 at Mount Stromlo. In each object, signal was summed in the spatial direction and sky subtraction accomplished by subtracting from this sum signal in parts of the slit which were uncontaminated by field H II emission.

Observations of the two SNRs in the LMC and in our Galaxy were made on the nights of 1977 December 7 and 1978 April 1, respectively, using the 3.9 m Anglo-Australian Telescope. The spectrograph was the Royal Greenwich Observatory f/7.9 Cassegrain instrument with its grating #4. The detector was the AAT image photon-counting system (Boksenberg 1972; Boksenberg and Burgess 1971). The slit was $180'' \times 2''$ aligned E-W in December and N-S in April, and signal was divided into six bins along the slit corresponding to a counting area per bin of 36 arcsec^2. Integrations were all 900 s, and calibration and reduction procedures were effectively identical to the SIT data.

Integrations of the M33 and M31 were all made with the slit passing through the brightness center of the object. However, for the more extended LMC and Galactic objects, brighter regions were selected. The slit center positions (epoch 1950.0) are as follows: N86: $04^h56^m07^s.9$, $-68°43'17''$. N206: $05^h32^m48^s.9$, $-71°02'24''$. RCW 86: $14^h36^m18^s.2$, $-62°25'36''$. RCW 103: $16^h13^m50^s.6$, $-50°59'12''$.

Figure 1 shows red sections of two SIT frames (unreduced except for some smoothing) for the two SNRs

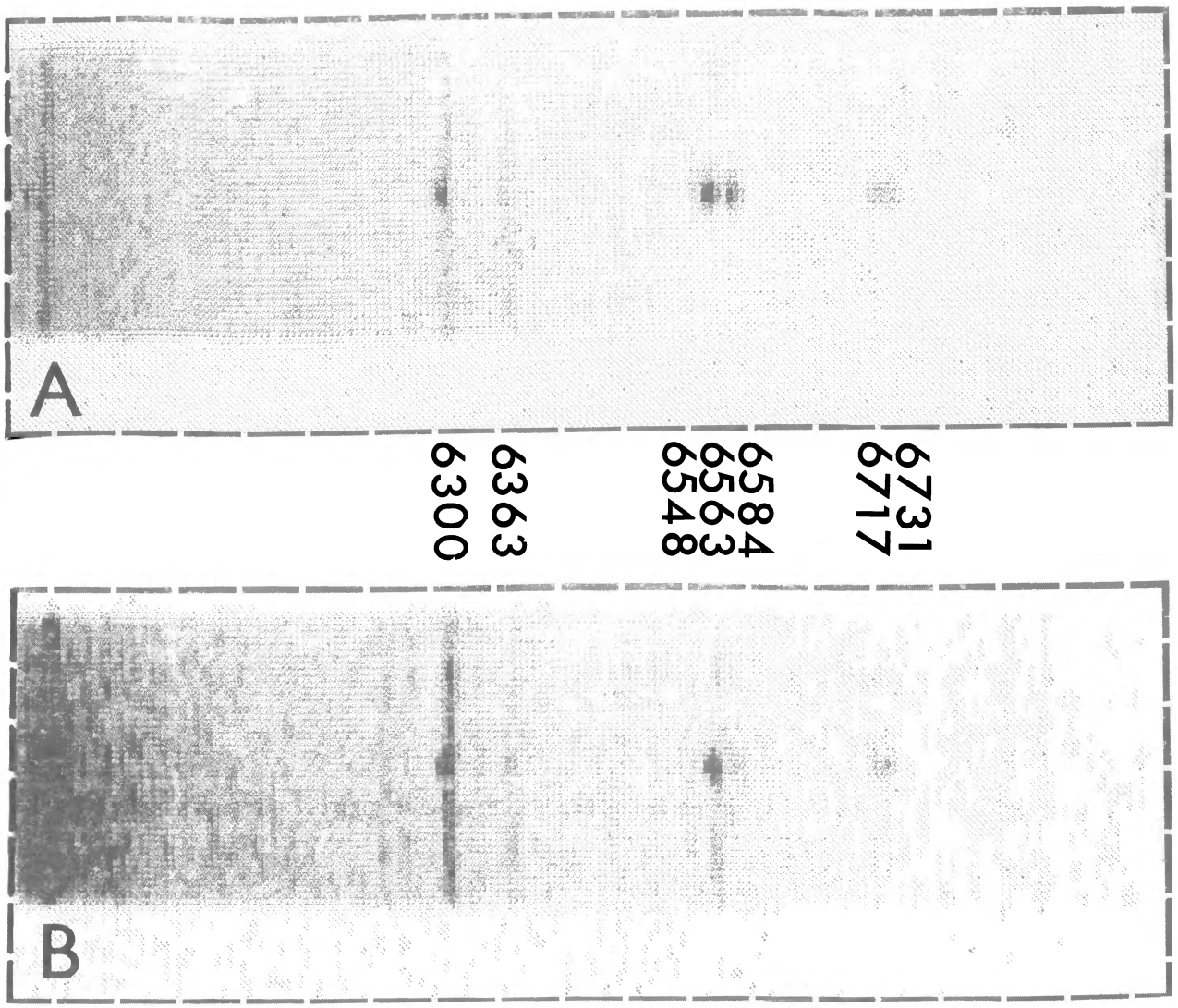

FIG. 1.—Red portions of two SIT frames of SNR in M33. These are unprocessed except for some smoothing in the spatial direction. Note the extreme difference in nitrogen line strength between A, M33 2-7, and B, M33 2-2. This is due, at least in part, to large-scale abundance gradients.

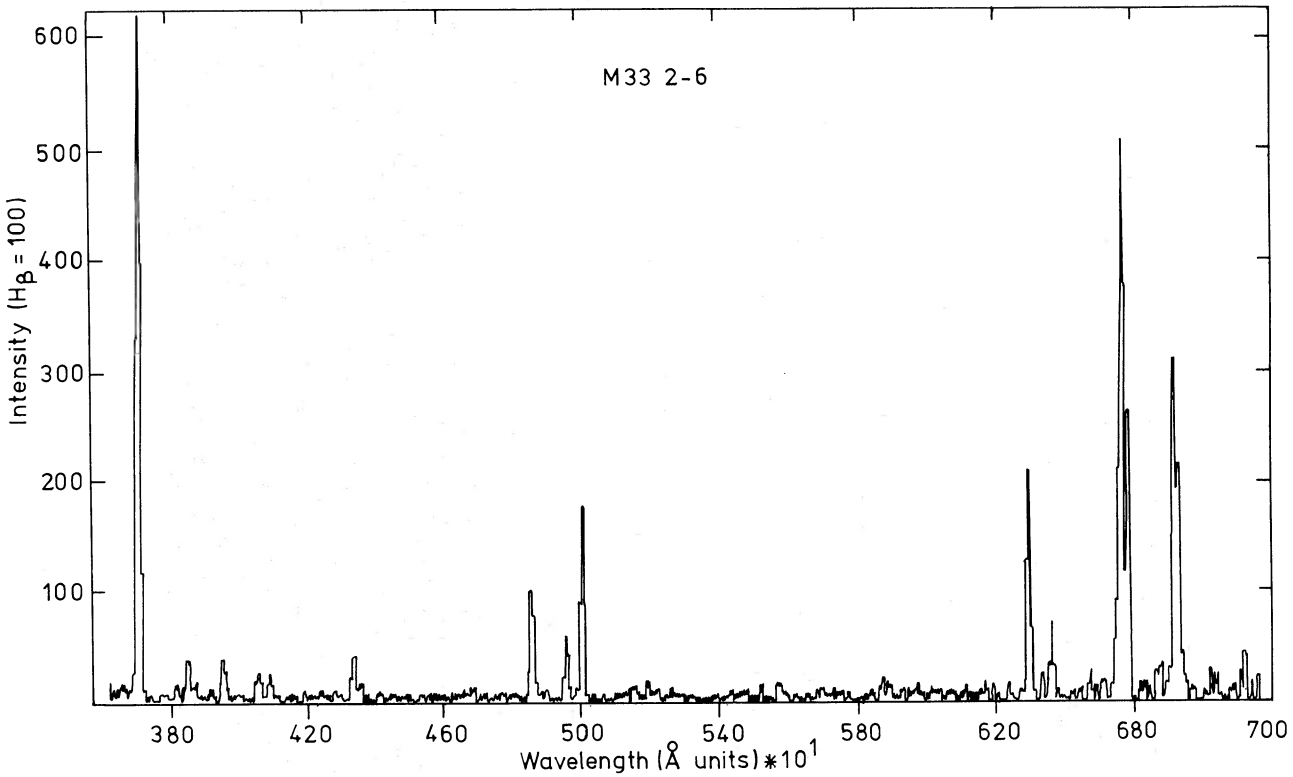

FIG. 2.—A fully reduced SIT frame for SNR M33 2-6. The signal-to-noise is typical of a well-exposed frame.

M33 2-7 and 2-2. Note the strong [O I] lines, [S II] (λ6731/λ6717) ratios above the low density limit of $\frac{2}{3}$, and the extreme difference in the [N II] λ6584 line intensities. This is the result of the abundance gradient between 2-7 (close to the center) and 2-2 (far from the center). A fully reduced SIT frame is shown in Figure 2, and the full spectral data are given in Table 1 for SNRs and in Table 2 for H II regions, where intensities are normalized to Hβ = 100 according to the standard practice. Because of the narrowness of the slits, no attempt has been made to derive absolute flux. Relative spectral intensities are probably not influenced by systematic errors due to atmospheric dispersion since all observations were made at a zenith distance not exceeding 50°, and for most of the M33 observations much less than this.

Note the severe differences between the spectrophotometry presented here and that of Danziger *et al.* (1978) for the first three SNRs discovered by D'Odorico, Benvenuti, and Sabbadin (1978). These objects, M33-1, M33-2, and M33-3, are those called here by their new catalog numbers M33 2-7, 2-8, and 2-9, respectively. Although the red portion of the spectrum shows tolerable agreement with the AAT and Asiago data, the [O II] lines are in very poor agreement. As these authors note, this is probably the result of uncertainties caused by atmospheric dispersion and atmospheric absorption at the very large zenith distance of their observations.

In our objects, spectral coverage is sufficiently complete to permit two independent determinations of reddening. The first is given from a least squares fit to the Hα/Hβ/Hγ/Hδ decrements. All models agree that, for complete preionization of the gas entering the shock, contributions by collisional excitation to the Balmer decrement are unimportant. Hence we can use the case B Balmer decrement computed by Brocklehurst (1971) at a density given by the ratio of the [S II] λ6731/λ6717 ratio (Pradhan 1976) and at a temperature of 7000–8000 K (the recombination temperature). To obtain the reddening constant, this theoretical decrement was compared with the observations assuming a Whitford (1958) reddening law.

The second method is derived from the observation that, in models, the density-sensitive [S II] line ratio mentioned above is a unique function of the [S II] blue to red line ratio (λ4067 + 4076)/(λ6717 + 6731). This function was given in Paper IV (Dopita 1978), where it was used to derive reddening in Herbig-Haro objects. From the values determined by these two methods, it can be seen that in SNRs they are generally in good agreement, and the reddening constant adopted is a weighted mean of that given by each.

III. DERIVATION OF ABUNDANCES

The shock conditions were determined principally from the density-sensitive [S II] λ6731/λ6717 ratio, and the predominantly temperature-sensitive ratios [O III] λ5007 to [O II] λ3726 + 3729 and [O III] λ5007 to [O I] λ6300. These ratios have been given as diagnostic plots in Paper II, with the modification that the [S II] ratio

TABLE 1A

OBSERVED RELATIVE FLUXES $I(\lambda)$ AND REDDENING CORRECTED FLUXES $F(\lambda)$ FOR M33 SNR

Object		M33 2-2		M33 2-4		M33 2-5		M33 2-6		M33 2-7		M33 2-8	
Ion	Å	I(λ)	F(λ)	I(λ)	F(λ)	I(λ)	F(λ)	I(λ)	F(λ)	I(λ)	F(λ)	I(λ)	F(λ)
[OII]	3728	490	504	437	577	559	910	657	1026	824	1340	520	687
Hθ	3835							-	-	-			
[NeIII]	3868	9	9	-	-	-	-	33	48	56	85	26	33
HeI, HI	3889	8	8	-	-	-	-	6	9	-	-	14	18
CaII	3934	-	-	-	-	-	-	7	10	-	-	-	-
NeIII He, CaII	3968	28	29	14	17	37	54	38	54	41	59	32	40
[SII]	4073	16	16	11	13	129	26	26	35	27	37	14	17
Hδ	4101	22	22	19	23	19	26	20	27	17	23	21	25
Hγ	4340	44	44	33	37	46	57	35	43	44	54	46	52
[OIII],[FeII]	4362	14	14	-	-	19	24	16	19	12	15	12.5	14
MgI	4562,71							6	7	-	-	-	-
HeII	4686	-	-	-	-	-	-	7	8	8	9	12	12
Hβ	4861	100 ± 5[1]		100 ± 6		100 ± 10		100 ± 2		100 ± 5		100 ± 4	
[OIII]	4959	41	41	38	37	54	52	56	54	138	133	81	79
[OIII]	5007	121	121	107	104	146	139	167	159	412	392	202	196
[FeII]	5158	9	9	-	-	-	-	12	11	5	5	7	7
[NI]	5199	-	-	-	-	12	10	16	14	5	5	7	6
[FeII]	5261,74	-	-	-	-	-	-	8	7	-	-	-	-
[NII]	5755	-	-	-	-	-	-	-	-	13	8	-	-
HeI	5876	-	-	-	-	-	-	14	10	32	23	15	12
[OI]	6300	60	58	50	38	182	114	186	120	162	101	57	43
[OI]	6363	28	27	7	5	64	39	53	34	56	34	11	9
[NII]	6548	17	16	30	23	54	32	90	55	160	94	53	39
Hα	6563	260	252	395	288	462	270	579	352	609	357	381	278
[NII]	6584	45	44	95	69	139	81	232	141	412	240	177	129
HeI	6678	-	-	-	-	36	20	26	15	25	14	13	9
[SII]	6717	134	129	160	114	355	200	246	145	240	136	161	115
[SII]	6731	105	102	90	65	295	167	230	135	290	164	139	100
C_{Bal}	-	0.00	0.04	0.48	0.41	0.57	0.7	0.83	0.65	0.96	.7	0.37	.41
C_{SII}	-	0.08	±0.04	0.34	±0.1	0.87	±0.2	0.47	±0.2	0.46	±.2	0.46	±.05

[1]The formal error for this line is the measurement error, and does not take account of systematic errors which may reach 15%. Due to quantum efficiency variations, measurement errors rise both blueward and redward of Hβ. At Hα they are 3 times as great whereas at λ3728 Å they are 1.5 times as great.

TABLE 1B

OBSERVED RELATIVE FLUXES $I(\lambda)$ AND REDDENING CORRECTED FLUXES $F(\lambda)$ FOR M33 SNR

Object		M33 2-9		M33 2-11		M33 2-14		M33 2-15		M33 2-16		M33 2-18	
Ion	Å	I(λ)	F(λ)	I(λ)	F(λ)	I(λ)	F(λ)	I(λ)	F(λ)	I(λ)	F(λ)	I(λ)	F(λ)
[OII]	3728	696	834	727	1140	483	535	578	732	637	1760	782	1085
Hθ	3835	6	7	6	9					-	-		
[NeIII]	3868	39	45	22	32	22	24	47	57	10	24	32	42
HeI, HI	3889	18	21	14	20	-	-	12	15	-	-	10	13
CaII	3934	9	10	9	13	-	-	9	11	-	-	-	-
NeIII He, CaII	3968	36	41	35	49	14	15	37	44	29	63	27	35
[SII]	4073	17	19	32	43	11	12	15	17	11	22	13	16
Hδ	4101	22	25	26	35	25	27	25	29	16	31	24	29
Hγ	4340	51	55	41	50	43	45	39	43	38	60	45	52
[OIII],[FeII]	4362	9	10	8	10	10	10	15	17	-	-	21	24
[MgI]	4552, 71	-	-	-	-		-	-	-	5	6	-	-
HeII	4686	5	5	-	-	-	-	9	9	-	-	9	9
Hβ	4861	100 ± 4		100 ± 3		100 ± 6		100 ± 6		100 ± 5		100 ± 4	
[OIII]	4959	65	64	41	40	90	89	113	111	48	44	84	82
[OIII]	5007	175	172	123	117	243	240	248	254	130	117	234	226
[FeII]	5158	7	7	8	7	-	-	-	-	-	-	-	-
[NI]	5200	8	8	1717	15	-	-	6	6	15	11	-	-
[FeII]	5261,74	5	5	4	4	-	-	-	-	-	-	-	-
[NII]	5755	-	-	-	-	-	-	-	-	-	-	-	-
HeI	5876	12	10	-	-	-	-	13	11			-	-
[OI]	6300	92	77	200	129	43	39	53	42	132	49	75	55
[OI]	6363	25	21	72	46	15	14	12	9	60	21	31	22
[NII]	6548	50	41	50	31	31	28	38	30	97	32	42	29
Hα	6563	339	278	480	292	307	274	391	301	1030	337	382	267
[NII]	6584	160	131	188	114	81	72	104	80	235	76	122	85
HeI	6678	10	8	-	-	-	-	22	16	-	-	-	-
[SII]	6717	202	163	338	199	123	109	183	138	325	99	134	129
[SII]	6731	146	117	252	148	96	85	117	89	289	87	105	102
C_{Bal}	-	0.23	.26	0.56	0.39	0.10	0.15	0.37	0.34	1.46	1.46	0.35	0.47
$C_{[SII]}$	-	0.30	±.05	0.22	±0.2	0.31	±0.08	0.29	±0.10	1.46	± .1	0.85	±0.17

TABLE 1C

OBSERVED RELATIVE FLUXES $I(\lambda)$ AND REDDENING CORRECTED FLUXES $F(\lambda)$ IN GALAXIES OTHER THAN M33

Object		Galaxy RCW86		Galaxy RCW103		LMC N49*		LMC N86		LMC N206		M31 BA55	
Ion	Å	I(λ)	F(λ)	I(λ)	F(λ)	I(λ)	F(λ)	I(λ)	F(λ)	I(λ)	F(λ)	I(λ)	F(λ)
[OII]	3728	470.6	887	204	690	648	648	593	1124	712	1416	840	1059
Hθ	3835											-	-
[NeIII]	3868	33.8	58.3	22.9	64.9	45	45	11	19	7	12.6	64	78
HeI, HI	3889	12.4	21.1	7.4	20.4	27	27	8	13.8	8	14.2	-	-
CaII	3934	6.8	11.3	-	-	16	16	-	-	-	-	-	-
NeII He, CaII	3968	23.5	38.2	8.1	20.4	41	41	16	26	27	45.5	38	45
[SII]	4073	21.0	32.2	15.8	35.9	36.1	36.1	7.4	11.4	12	18.9	~30	~35
Hδ	4101	15.9	23.9	15.8	34.5	36.4	36.4	18	27.2	14	21.8	~16	18
Hγ	4340	34.0	45.0	26.3	44.7	51.5	51.5	34	45.0	31	41.8	46	52
[OIII],[FeII]	4362	14.3	18.8	10.0	16.7	7	7	12	15.9	4	5.4	16	18
[MgI]	4552,71											-	-
HeII	4686	5.8	6.4	7.5	8.9	8.5	8.5	-	-	-	-	~14	~14
Hβ	4861	100 ± 0.8		100 ± 1.7		100	100	100 ± 3.9		100 ± 5.0		100 ± 12	
[OIII]	4959	74.2	71.3	79.4	73.0	39.8	39.8	60.6	58.0	30	28.7	109	107
[OIII]	5007	222.6	208.5	256	226	95.5	95.5	189	177.0	85	79.2	271	264
[FeII]	5158	5.9	5.1	16.3	12.4	17.5	17.5	-	-	-	-	-	-
[NI]	5200	7.8	6.6	35.2	25.7	8.3	8.3	-	-	(8)	(6.7)	~15	~14
[FeII]	5261,74	3.9	3.2	11.0	7.6	6.8	6.8	-	-	-	-	-	-
[NII]	5755	5.9	3.9	21.4	9.8	-	-	-	-	-	-	-	-
HeI	5876	11.0	7.0	34.2	14.3	11.6	11.6	(15)	(9)	25	15	~22	19
[OI]	6300	191.3	103.3	354.8	110.1	123.7	123.7	40.6	22	165	85.3	127	102
[OI]	6363	55.1	29.2	118.9	35.5	43.5	43.5	14	7.5	54	27.2	42	34
[NII]	6548	170.6	85.2	612	163	30.6	30.6	31	15.5	45	21.4	183	142
Hα	6563	621.5	308.3	1086	285.6	295.8	295.8	651	322.2	637	300	450	350
[NII]	6584	526.9	259.7	1830	475.6	77.1	77.1	95.7	47.2	122	56.9	558	433
HeI	6678	6.5	3.1	13.3	3.3			9.5	5.6	6.8	3.1	-	-
[SII]	6717	227.6	107.8	479	115.3	172	172	172	53.2	214	95.9	330	272
[SII]	6731	276.7	130.5	621	148.3	190	190	120	37.2	166	74.2	205	169
C_{Bal}	-	0.915 ± 0.20	0.917	1.67	1.75 ± 0.15	0.0		1.01	0.92	1.08	0.98	0.50	.33
C_{SII}	-	0.920 ± 0.09	±0.101	1.83		0.0		0.72	±0.15	0.70	±0.17	0.17	±.15

* Taken from Osterbrock and Dufour, 1973

TABLE 2

OBSERVED RELATIVE FLUXES $I(\lambda)$ AND REDDENING CORRECTED FLUXES $F(\lambda)$ FOR H II REGIONS IN M33

Ion	Å	NGC 604		B 749		B 77		B 710		B 214		NGC 595		NGC 588	
		I(λ)	F(λ)	I(λ)	F(λ)	I(λ)	F(λ)	I(λ)	F(λ)	I(λ)	F(λ)	I(λ)	F(λ)	I(λ)	F(λ)
[OII]	3728	177	210	316	411	176	255	303	451	248	419	175	279	104	120
[NeIII]	3868	8.5	9.8	-	-	4	5.5	4.6	6.4	-	-	3.5	5.2	21.9	24.8
HeI, HI	3889	10.5	12.1	11	14	12.8	17.5	7	9.7	-	-	14.7	21.4	10.8	12.2
[NeIII], He,	3968	23.7	27.0	16.5	19.8	18.9	25.0	17	23	-	-	16.5	23.5	28	31.3
[SII]	4068,76	2.7	3.0	-	-	-	-	-	-	-	-	-	-	-	-
Hδ	4101	21.9	24.4	21.6	25.6	22.3	28.3	19.5	25.2	19.4	27.1	22.5	30.4	21.7	25.0
Hγ	4340	43	46.3	46.2	51.8	39.5	46.5	40.3	47.9	39.5	49.6	39.5	48.4	52.0	55.4
[OIII]	4363	≲2.0	≲2.15	-	-	-	-	-	-	-	-	≲0.8	≲1.0	3.3	3.5
Hβ	4861	100 ± 1.0		100 ± 3.5		100 ± 1.5		100 ± 1.5		100 ± 3		100 ± 0.8		100 ± 0.6	
[OIII]	4959	67.1	66.4	9.3	9.1	21.5	21.0	30.2	29.4	14.8	14.3	50.6	49.1	170.8	169.2
[OIII]	5007	175.6	172.6	39	37.9	66.8	64.3	86.8	83.3	50.3	47.7	145.5	138.7	448	441.5
HeI	5876	14.8	13.1	14.9	12.3	16.5	12.7	13.5	10.2	15	10.3	15.5	11.1	14.5	13.1
[OI]	6300	-	-	10	7.7	-	-	(6)	(4)	-	-	-	-	-	-
[NII]	6548	10.4	8.6	20.4	16.7	24	18.2	20	14.8	42	23.8	22.7	13.7	4.8	4.1
Hα	6563	337.2	279.7	395	295	443	295	444	287	530	298	504	302	341	290.4
[NII]	6584	28.8	23.8	71.2	53.2	93	61.7	77.2	49.7	105.7	59.0	81.4	48.5	131	11.1
	6678	4.9	4.0												
[SII]	6717	32.9	27.0	33.1	24.3	33.5	21.7	39.5	24.8	54.5	29.4	25.1	14.5	21	17.7
[SII]	6731	17.6	15.3	28.8	21.1	28.0	18.6	31.5	19.7	52.0	28.0	16.5	9.5		
C_{Bal}	6717	0.24	±0.04	0.38	±0.10	0.53	±0.08	0.57	±0.06	0.75	±0.09	0.67	±0.10	0.21	±0.12
N^+/S^+	6731	3.79		7.62		9.80		7.17		7.13		12.57		4.25	

density scale has been multiplied by a factor 0.48 to correct to the newer collision strengths of Pradhan (1976).

It must be noted that the preshock density and shock velocity so derived may not be correct because of the neglect of magnetic field pressure and because the temperature-sensitive line ratios become insensitive to the shock velocity when this is above about 120 km s^{-1}. However, these parameters enter into the abundance analysis only at second order, so high accuracy is not required. In some cases a more accurate estimate of the shock velocity can be obtained from the [N II] lines. Raymond (1976) showed that, for velocities greater than about 100 km s^{-1}, there is a good correlation between shock velocity and the ratio [N II] $\lambda 6548 + 6584/\lambda 5755$ in the sense that this becomes larger as the shock velocity increases.

To those who use this ratio to measure electron temperatures in H II regions this result must seem somewhat paradoxical, since higher temperatures give lower values of this ratio. The physical reason for the computed correlation is that, above 100 km s^{-1}, photoionization of the recombination zone by photons produced near the shock front starts to become important (compare Shull and McKee 1979). This produces a more extended recombination zone at low temperature ($< 10{,}000$ K) which lowers the mean temperature of the [N II] emitting region.

Shock conditions having been obtained abundances of O, N, and S were obtained by simple application of the methods of Paper II. Again correction has to be made in the case of sulfur: abundances implied by Paper II must be multiplied by a factor 1.2. At high velocities the [O III] lines $\lambda\lambda 4959, 5007$ tend to be independent of shock conditions, but are affected by the abundance of carbon. Here, the observed intensity of these lines has been used with an assumed C/O abundance ratio of $\frac{1}{3}$ to give an independent estimate of oxygen abundance from Figure 9 of Paper II. A third abundance estimate for oxygen is given by the [O I] line at 6300 Å. Since this line is not generally the major coolant in the recombination zone where it is produced, we assume that its strength is proportional to the oxygen abundance and has an intensity relative to Hβ of 0.8 at an oxygen abundance of 2×10^{-4}, a value derived from the shock models. This latter estimate probably has lower accuracy than the other two because it is more affected by the photoionization in the recombination zone. The large scatter in the oxygen abundance for Magellanic Cloud SNRs found in Paper III is probably caused by this effect. In this paper, the adopted oxygen abundance is simply the mean of the three estimates.

The neon abundance can be estimated, as in H II regions, by comparing the [Ne III] $\lambda 3868$ line with the [O III] $\lambda 5007$ line. Both are produced in a hot ($3\text{–}8 \times 10^4$ K) zone. Raymond's (1976) models show that over a wide range of shock conditions and relative abundances:

$$\frac{I_{5007}}{I_{3868}} = 1.44 \frac{Z(\mathrm{O})}{Z(\mathrm{Ne})} .$$

This was used to derive the neon abundance. The accuracy of these determinations is probably a factor 1.5 times lower than the oxygen abundance.

Because the hydrogen and singly ionized helium recombination coefficients are very similar, the fractional ionization of these two ions is very similar in the recombination zone. Furthermore, Shull and McKee (1979) show that, for shock velocities greater than 110 km s^{-1}, helium and hydrogen are fully preionized in the self-consistent model. This condition is probably satisfied in all the SNRs for which He I $\lambda 5876$ was observed with the possible exception of N206. It is probably safe to assume that the bulk of the recombination emission arises in the recombination zone of the shock structure, so to obtain the total helium abundance the recombination-cascade calculations of Brocklehurst (1971, 1972) can be used with a recombination temperature of 8000 K (Paper II). This gives

$$\frac{I_{5876}}{I_{\mathrm{H}\beta}} = 1.35 Z(\mathrm{He})$$

and

$$\frac{I_{6678}}{I_{\mathrm{H}\beta}} = 0.37 Z(\mathrm{He}) .$$

The adopted helium abundance is derived from the first of these ratios. The 4686 Å line of He II is less reliable as a measure of helium abundances, since it depends critically on the shock conditions, namely the ionization level achieved in the shock and the degree of preionization, and also on the relative importance of the collisional excitation and recombination-cascade processes. However, in one or two cases where the shock velocity is thought to be accurate, the Raymond (1976) models have been used to estimate the helium abundance (given as bracketed values in Table 3).

The accuracy of the helium abundances derived in this paper for the M33 SNR is rather unsatisfactory. Measurement errors for the 6678 Å line are, where given, 30–50% due to the low quantum efficiency of the SIT tube at this wavelength, and the 5876 Å line is perturbed by the proximity of the Na D lines at this low dispersion, which are strong in the Palomar night sky.

Table 3 gives a summary of the abundances obtained with the above considerations from the data of Table 1.

IV. WHAT DOES ABUNDANCE MEASURE?

In the Introduction we gave the many limitations of H II regions as abundance tracers in the interstellar medium. Our discussion would not be complete, therefore, without consideration of what intrinsic problems are connected with using SNRs to do the same job.

a) Contaminated by Supernova Ejecta

A common misapprehension about SNR spectra is that these are more likely to furnish abundances of the supernova ejecta than of the interstellar medium.

TABLE 3

DERIVED SHOCK CONDITIONS AND ABUNDANCES IN SNRs

Object	log N_1	T_2	Z(S)	Z(N)	Z(O) [OII]	Z(O) [OI]	Z(O) [OIII]	Z(O)	Z(Ne)	Z(He)[3]
M33 2-2	0.5	1.3E5	2.60E-6	0.72E-5	1.06E-4	1.45E-4	1.25E-4	1.25E-4	1.34E-5	-
M33 2-4	<0.6	>1.5E5	2.28E-6	1.04E-5	1.24E-4	0.95E-4	0.89E-4	1.03E-4	-	-
M33 2-5	1.0	9E4	7.00E-6	1.88E-5	3.02E-4	2.85E-4	(3.78E-4)	3.10E-4	-	-
M33 2-6	1.4	8E4	3.56E-6	3.40E-5	3.95E-4	3.00E-4	3.20E-4	3.37E-4	1.47E-4	-
M33 2-7[1]	<1.0	>2E5	5.28E-6	8.27E-5	6.50E-4	2.50E-4	3.30E-4	4.10E-4	1.28E-4	0.17 (0.18)
M33 2-8	<1.0	>2E5	3.00E-6	2.37E-5	1.90E-4	1.60E-4	1.70E-4	1.73E-4	4.20E-5	0.09 (0.13)
M33 2-9	<0.9	1E5	3.00E-6	2.60E-5	2.55E-4	1.93E-4	2.24E-4	2.24E-4	8.40E-5	0.07
M33 2-11	<0.5	7E4	5.28E-6	2.68E-5	3.42E-4	3.22E-4	3.18E-4	3.27E-4	1.29E-4	-
M33 2-14	1.0	1E5	3.80E-6	1.24E-5	1.20E-4	0.98E-4	(3.60E-4)	1.59E-4	(2.29E-5)	-
M33 2-15	<0.4	>3E5	2.84E-6	1.45E-5	1.79E-4	1.05E-4	2.17E-4	1.67E-4	5.40E-5	0.08
M33 2-16[2]	≈0.9	.6-1.5E5	(6E-6)	3.2 E-5	13.6 E-4	1.2 E-4	1-3E-4	(1.5 E-4)	(1.3 E-5)	-
M33 2-18	<0.4	>3E5	5.48E-6	1.54E-5	3.91E-4	1.37E-4	1.93E-4	2.40E-4	6.4 E-5	- (0.15)
M31 BA55	<0.5	1.4E5	1.2 E-5	1.26E-4	4.50E-4	2.60E-4	2.40E-4	3.20E-4	1.40E-4	0.14 (0.16)
LMC N49	1.6	8E4	5.4 E-6	1.46E-5	1.85E-4	3.09E-4	1.90E-4	2.10E-4	1.42E-4	0.086(0.126)
LMC N86	<1.0	>9E4	1.9 E-6	1.68E-5	3.50E-4	0.55E-4	4.08E-4	2.70E-4	4.18E-5	0.101
LMC N206	0.8	7E4	4.92E-6	1.26E-5	7.0 E-4	2.13E-4	1.40E-4	3.50E-4	8.02E-5	0.097
RCW 86	1.6	1.3E5	4.08E-6	6.20E-5	2.78E-4	2.57E-4	2.50E-4	2.62E-4	1.05E-4	0.087
RCW 103	1.5	1.4E5	4.90E-6	8.84E-5	2.20E-4	2.80E-4	2.10E-4	2.36E-4	9.76E-4	0.097(0.104)

[1] Some evidence for enrichment by SN ejecta.

[2] Spectrum affected by photoionisation in NGC604, diagnostic technique does not give consistent results.

[3] Helium abundances for M33 of low reliability, see text.

In fact this can easily be shown to be incorrect in the majority of cases by considering the radius at which a supernova blast wave has interacted with a mass of interstellar material at least an order of magnitude greater than that ejected, since the ejecta can show a heavy-element abundance by mass about an order of magnitude greater than that existing in the interstellar medium. If n is the density of the interstellar medium and the supernova ejects about 3 $M_\odot$, then this condition is satisfied at radius $r = 7(n\ \mathrm{cm}^{-3})^{-1/3}$ pc. For a canonical value of $n = 1\ \mathrm{cm}^{-3}$ all the M33 SNRs in Table 4 should have swept up more interstellar medium than has been ejected.

In practice, the situation is a little more complex than this. Cas A is perhaps the best example of a young SNR in our own Galaxy which shows abundance anomalies. Applying the above condition, we find that this SNR has interacted with 0.1–1 $M_\odot$ of interstellar gas (according to whether the density is 0.1 or 1.0 cm^{-3}, respectively. This SNR shows two distinct components. One consists of quasi-stationary flocculi (QSF) with a velocity dispersion of $\sim 200\ \mathrm{km\,s}^{-1}$ and an expansion velocity (from proper motions) about 150 $\mathrm{km\ s}^{-1}$ (Kamper and van den Bergh 1976). The other component is in fast-moving knots (FMK) with space velocities 4140–8460 $\mathrm{km\ s}^{-1}$ which appear to have originated from a common center at between A.D. 1653 and A.D. 1671 (Kamper and van den Bergh 1976). The FMK seem to be ejected material with very high O, Ar, and S abundances and no apparent He and H (Kirshner and Chevalier 1978; Chevalier and Kirshner 1978). Such a mix of material is predicted to occur in the zone just outside the core of a 15 $M_\odot$ model star just prior to collapse (Weaver, Zimmerman, and Woosley 1978). These knots have relatively high density ($\sim 10^4\ \mathrm{cm}^{-3}$) and are probably formed by instabilities which occurred shortly after the explosion (Chevalier 1975). Some of the ejecta must therefore be regarded as interacting with the interstellar gas in a "grapeshot" way rather than as a homogeneous bubble. The QSF can be explained as shocked cloudlets, but an apparent overabundance of nitrogen in them suggests that they too are contaminated by stellar material, and the low expansion velocities probably require them to have been formed in a pre-supernova mass-loss phase.

Two other objects in our Galaxy seem to offer evidence that such a phase can occur. The ring nebula NGC 6888 around the WN6 star HD 192163 with a radius of about 3 pc shows a distinct overabundance of nitrogen in the nebula (Parker 1978). The N:O abundance ratio is about 1:2. The SNR Pup A also shows a nitrogen abundance anomaly which is probably greater than this. Here individual filaments seem to have core N abundances higher than halo values, showing the extent to which the interstellar medium has modified the original ejecta.

To this evidence that the ejecta forms dense knots we must also add observational evidence that the normal interstellar medium is cloudy. In the LMC the properties of these cloudlets has recently been inferred both indirectly and directly from observations of evolved SNRs (Dopita 1979; Dopita and Mathewson 1979). The cloudlets have an average atom density of 10–20 cm^{-3} and are about 0.5 pc in diameter, which implies a mass of about 0.03 $M_\odot$. Such cloudlets are the natural consequence of an interstellar medium dominated by the effects of supernova shocks (McKee and Ostriker 1977). When a cloudlet is immersed in the hot post–blast-wave gas, a slow shock is driven into it by the surface pressure, giving the characteristic spectrum. A pessimistic estimate for the point at which this spectrum is contaminated by the ejecta is obtained by demanding that the mass of the cloudlet be at least 10 times the mass of the ejecta expelled in the solid angle subtended by the cloudlet at the supernova. This gives the minimum cloudlet distance $r = 5.0(nr_c)^{-1/2}$pc, where r_c is the cloudlet radius in parsecs and n is its density in H atoms cm^{-3}. This is only 1.8 pc for a cloudlet of the above parameters, showing that a cloudy interstellar medium makes contamination of the optical spectrum by the ejecta less likely than in uniform-density cases. In the X-ray frequencies, however, abundances may reflect those of the ejecta because in a cloudy interstellar medium (ISM), these remain hotter. In M33, which is likely to have a structure of the interstellar medium similar to the LMC (D'Odorico, Dopita, and Benvenuti 1979*b*), only one SNR appears to suffer appreciable enrichment by the ejecta. This is #2-7 (#1 of D'Odorico, Benvenuti, and Sabbadin 1978, incorrectly classified as a W-R star by Wray and Corso 1972). This shows appreciably larger N and He abundances than the others, even those closer to the galactic center, has a small diameter (6 pc), and occurs in an interarm region where the mean interstellar density is probably lower. Furthermore, Danziger *et al.* (1979) find that the [O III] line shows a two-component structure with a sharp core and an extended halo with velocity dispersion $\sim 10^3\ \mathrm{km\ s}^{-1}$. This is reminiscent of Cas A and the

TABLE 4

POSITIONS AND SIZES OF THE SNR IN M33

SNR	r (kpc)	R (kpc)	d (pc)
2, 1.....	2.48	4.37	65
2, 2.....	2.46	4.16	7
2, 3.....	2.87	3.80	17
2, 4.....	2.17	3.72	18
2, 5.....	3.05	3.05	17
2, 6.....	1.14	2.02	9
2, 7.....	1.49	1.58	6
2, 8.....	0.58	0.78	11
2, 9.....	1.26	1.55	7
2, 10.....	3.74	4.23	42
2, 11.....	1.02	1.34	7
2, 12.....	2.83	2.83	22
2, 13.....	2.98	2.99	35
2, 14.....	1.70	2.87	46
2, 15.....	1.71	2.89	20
2, 16.....	2.42	2.98	6
2, 17.....	2.09	3.65	54
2, 18.....	2.31	3.43	39
2, 19.....	2.47	3.85	24

NOTE.—Columns give identification, projected distance from center, deprojected distance, and diameter of SNR.

QSF–FMK dichotomy. In any event we find, as they did, that the [O III] lines are too strong in comparison to the [O I] than is allowed by simple shock models. This may indicate the effect of strong [O III] emission from the high-velocity medium.

b) *The Fate of Dust*

Nitrogen offers perhaps the best element to trace the fate of the volatile "dirty ices" because it forms, unlike S and O, virtually no refractory grain compounds. Dopita (1977*b*), using observations by D'Odorico and Sabbadin (1976) and Daltabuit, D'Odorocio, and Sabbadin (1976), found that a systematic variation in the [N II]/Hα ratio was best explained in terms of destruction of N containing volatiles by sublimation by the supernova radiation pulse. Empirically, all these volatiles are returned to the gaseous phase inside a diameter 20–30 pc, which includes nearly all the M33 SNRs observed. In any event, this effect, although present in the LMC, is much less marked than in the Galaxy—possibly because of lower volatile "ice" grain abundance resulting from higher destruction rates. Since abundances in M33 and the LMC are broadly similar, as are supernova rates per unit mass of gas (D'Odorico, Dopita, and Benvenuti 1979*b*), we can probably safely assume that volatiles are all returned to the gas phase.

The question of the more refractory grains is more confused. For silicates, two recent papers suggest that magnetic field compression in the shock, by increasing the grain gyromotion, can increase sputtering sufficiently to effectively destroy these grains (Cowie 1978; Shull 1979). These authors differ slightly in estimating the critical shock velocity required to do this, but it probably lies between 70 and 100 km s^{-1}. Again the M33 SNRs fulfill this condition.

Graphite grains need higher velocities for sputtering to be efficient (as do ice grains if they are not destroyed by sublimation). However, recent UV observations show that, in the Cygnus Loop, carbon is progressively returned to the gas phase through the shock structure (Benvenuti, D'Odorico, and Dopita 1979). The shock velocity is only about 120 km s^{-1}, so some other destruction process must be involved.

Carbon, although important in the UV, has little effect on the visible lines except to produce a slight weakening of these at high abundance (Paper II). The only consequences of differential depletion effect similar to that seen in Cygnus is to enhance the [O III] lines by 10% and the [Ne III] lines by 40%.

c) *Limitations of the Modeling*

There are now three detailed sets of radiating shock wave models in the literature, those of Dopita (1977*a*, Paper II), Raymond (1976, 1979), and Shull and McKee (1979). Although Dopita has been the only author to systematically investigate the dependence on abundance, the models of Raymond extend to higher velocity. In this regime, they are probably more accurate because he considers in more detail the effect of ionizing photons (generated in the hot postshock gas) on the recombination zone. Shull and McKee have solved the preionization problem and give self-consistent models in which the preionization is set by the ionizing photons generated in the cooling zone. These models are particularly useful at low shock velocity.

In Table 5 we compare the abundance implied by these three sets of models for the galactic SNR RCW 103. Since all abundances are near solar values, we have simply assumed that line intensity is proportional to abundance to correct their models to our observations (except for the Dopita models). Despite the different assumptions and sets of atomic parameters, the maximum range in abundances are 0.22, 0.31, 0.36, and 0.50 in the logarithm for He, O, N, and S, respectively. This is rather satisfactory and gives cause for confidence that modeling errors may only account for a scatter of order 0.3 in the log of the absolute abundance. The SNR chosen for the comparison above is a rather fast ($V \sim 130$ km s^{-1}) shock, and also abundances are higher than the mean of the set observed here. Much of the disagreement between models can be accounted for by the differing way in which the transfer of ionizing UV photons produced in the cooling zone is treated. The Raymond models tend to overestimate the importance of this whereas the Dopita models underestimate the effect. The Shull and McKee model is probably most reliable since the transfer problem is treated in a self-consistent manner. At low metal abundance, this effect is much less important, and for the LMC SNR N49 the Raymond and Dopita models are in close agreement as far as O and N abundances are concerned.

Apart from this effect, two specific differences seem to be important, the cause of which is not clear. First, the Raymond models seem to underestimate the strength of the [S II] lines; second, the Shull and McKee models overestimate the [N I] lines. Since both these are emitted to an important degree in the cool gas which is only partially ionized, some of these differences

TABLE 5

COMPARISON OF MODELS FOR RCW 103

Model	Z(O)	Z(N)	Z(S)	Z(Ne)	Z(He)
Dopita	2.36E−4	8.84E−5	4.90E−6	(9.76E−5)	0.097 (0.104)
Raymond	4.90E−4	2.02E−4	1.58E−5	2.02E−4	0.058 (0.120)
Shull + McKee	3.50E−4	1.86E−4	6.91E−6	(1.45E−4)	0.057 (0.080)
Mean	3.59E−4	1.59E−4	9.20E−6	1.48E−4	0.086

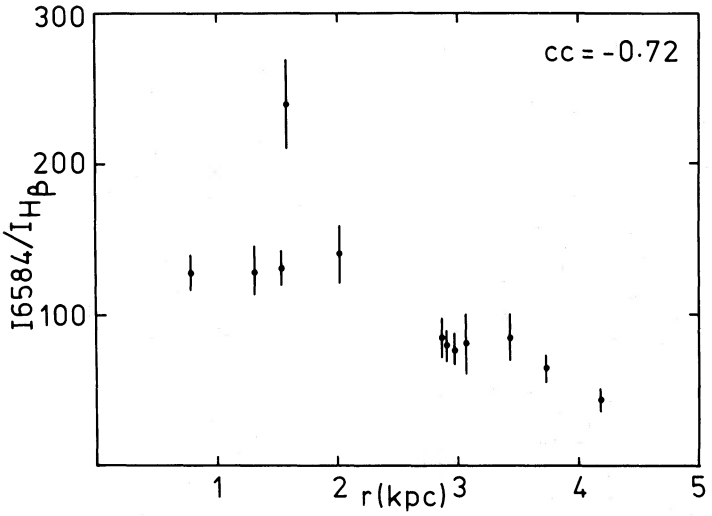

FIG. 3.—The [N II] 6584/Hβ ratio for SNR as a function of galactocentric distance in M33. This ratio is a very good abundance tracer since it is almost independent of shock conditions in SNRs.

could arise from divergence between models in their treatment of the infrared cooling.

Even for perfect modeling, uncertainties in the important atomic constants could introduce an error in the absolute abundance of 0.1 in the logarithm.

V. THE ABUNDANCE GRADIENT IN M33

Since the [N II] lines are very little affected by any shock parameter other than the nitrogen abundance, their intensity can be used as a very handy empirical abundance trace. Figure 3 shows the variations of the [N II] λ6584 A to Hβ ratio as a function of galactocentric distance proving the reality of an abundance gradient in M33. Note the anomalous position of M33 2-7 noted above, and the way in which the points at $r \sim 3$ kpc cluster, showing that neither diameter nor position angle of the SNR in the Galaxy is an important variable in determining this relationship.

Absolute abundance gradients of N and O are shown in Figure 4 with the correlation coefficient between $\log Z$ and r. The bars represent the difference between abundance values given here (lower extremity) and the likely abundance given by a Raymond (1976, 1979) model, estimated by interpolation of his models. As mentioned above, the true gradient probably lies between these extremes. Note that the gradients in N and O are virtually identical between 2.9 and 4.2kpc, amounting to $d(\log Z)/dr = -0.25\ \mathrm{kpc}^{-1}$. However, the gradients in the 1–3 kpc zone differ. For N it is (neglecting M33 2-7) $-0.18\ \mathrm{kpc}^{-1}$ whereas for O it is $-0.08\ \mathrm{kpc}^{-1}$. This will be discussed later.

Figure 4 should be interpreted with a certain amount of caution. The method of identification of SNR candidates naturally discriminates against discovery of large-diameter SNRs at small galactocentric distance. However, it is thought that very few SNRs with diameters less than 25 pc have been missed, since the distribution of these with radius is very similar to the distribution of supernovae with radius in Sc galaxies (Iye and Kodaira 1975). SNRs with large diameters may not have shocks powerful enough to destroy dust (§ IV*c*, above), so the gradient in Figure 4 may be steepened by inclusion of these objects, though there is little evidence to support this conjecture.

The inclusion of small-diameter ($r < 5$ pc) SNRs may certainly be questioned in view of the possibility of enrichment by the supernova ejecta (§ IV*a*, above). If these are excluded from the figure, the correlation between the O/H ratio and galactocentric distance

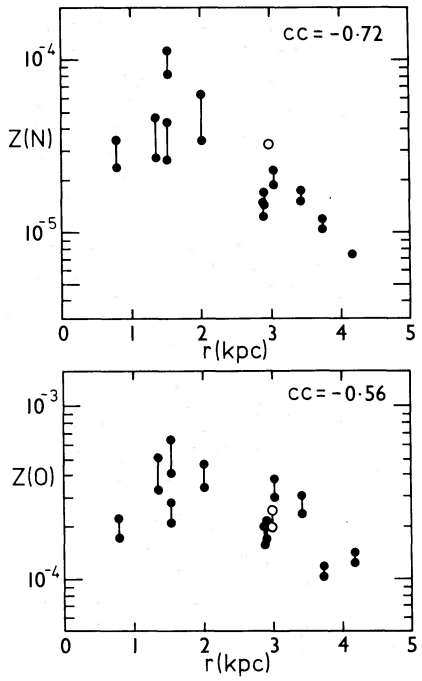

FIG. 4.—The absolute abundance gradients in nitrogen and oxygen in the arms of M33 as determined by SNRs. The length of the bars indicates likely errors due to modeling.

becomes rather weak. However, it is shown elsewhere (D'Odorico, Dopita, and Benvenuti 1979*b*) that the cumulative number/diameter relationship for SNRs in M33 is similar to that of the LMC and dissimilar to that of the Galaxy. Since in Paper V we have argued that the LMC relationship is a consequence of an extremely cloudy interstellar medium—a conclusion supported by [Fe XIV] observations (Dopita and Mathewson 1979) and new X-ray observations (Long and Helfand 1979)—it is likely that this conclusion also applies to M33. Thus, at worst, the lower limit of 1.8 pc for serious contamination of the spectrum by supernova ejecta applies. In practice, the cloudy ISM will ensure a very rapid expansion of the ejecta in the high-temperature X-ray emitting phase, while the slow shocks producing the optical emission will reflect accurately the composition of the cloudlets. Thus, only in the event of severe presupernova mass loss will our abundances be seriously compromised by the precursor star.

The simplest theory of chemical evolution (Searle and Sargent 1972) assumes that each zone of a galaxy evolves in isolation, from primordial abundance with an invariant initial mass function. In the instantaneous recycling approximation, an element with constant yield Y will have an abundance Z given by

$$Z = Y \ln (1 + M_s/M_g) ,$$

where M_s is the mass of stars formed and M_g the mass of gas remaining. Provided that the contribution of mass by H_2 is not too important, the surface density of H I can be used instead of M_g. The observations of Rogstad, Wright, and Lockhart (1976) are probably best for this. The surface mass of the stars can be obtained either through surface photometry (de Vaucouleurs 1959) or, better, from a rotation model (Bosma 1978). The resulting predictions of the simple theory are shown in Figure 5, scaled so that it fits the observations of the oxygen abundance at $r = 3$ kpc. It fails: the abundance gradient is lower than observed, an effect already familiar from H II region observations (Pagel 1978).

A recent variant of the simple theory allows the star formation rate to be a power of the local gas density, as suggested by Schmidt (1959):

$$\frac{d\sigma_g}{dt} = -C\sigma_g{}^n ,$$

where σ_g is the surface density. The exponent n seems to have a value between 1.6 and 1.8 in the SMC (Snaduleak 1969; van Genderen 1969). Talbot and Arnett (1975) compute models incorporating this idea and taking into account that, in a disk system, star formation produces depletion of gas in the $z = 0$ plane, so the infall rate must also be considered. This model is also shown on Figure 5. This helps to produce a steeper gradient in the outer parts of M33, but predicts an abundance peak at about 2.5 kpc. Such an effect is not excluded by the SNR observations, but does not seem likely if the H II region

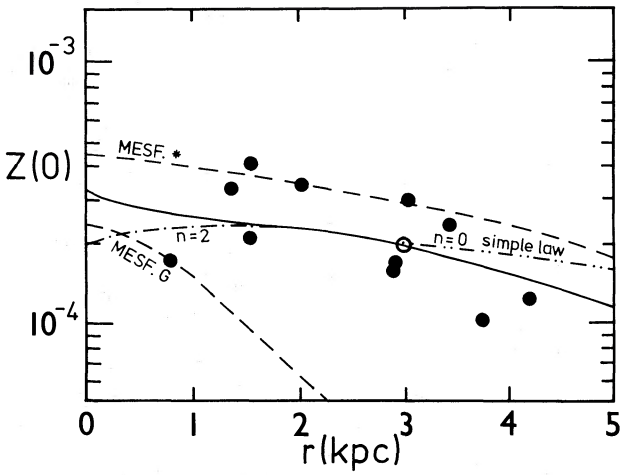

FIG. 5.—The absolute N/S gradient in M33 as determined from SNR (*rings*) and H II regions of low excitation (*triangles*). Lines connect SNR and H II regions which are (spatially) near to one another.

results are to be believed (Benvenuti, D'Odorico, and Peimbert 1973). However, in M33 the exponent n is not constant. Madore, van den Bergh, and Rogstad (1974) find that $n = 2.4$ would fit in the region exterior to 2.5 kpc, but that in the inner region $n =$ 0.4–1.0. A compound law which changes from the Talbot and Arnett model to a simple law at 2.5 kpc is probably more realistic.

Metal-enhanced star formation (Talbot and Arnett 1975) is excluded, at least in their formulation of the effect. Although the trend and absolute value of the abundance predicted for the stars is in tolerable agreement with the observations, the gas abundance gradient prediction is far too steep (Fig. 5). The possibility that the star formation process is influenced by the metallicity of the gas is not disproved, but it is less critical to this parameter than the simplified Talbot (1974) formulation.

Although the dual power law model seems to give a reasonable fit to the run of enrichment with radius, it still seems to be not quite steep enough in the 3–5 kpc zone. This could be due to an increase in the z thickness of the gas disk implied by the velocity dispersion. Warner, Wright, and Baldwin (1973) estimate that this goes from 300 pc near the nucleus to 800 pc in the outer part. Madore, van den Bergh, and Rogstad (1974) suggest that there would be a portion of the H I which does not participate in the star formation process, resulting in the apparent change in index.

We consider that a more sophisticated model is probably required, taking into account the halo evolution. Tinsley and Larson (1978) have built enrichment models based on galactic collapse models (Larson 1976), and Ostriker and Thuan (1975) consider the effect of pre-enrichment of the disk gas while most of it is still in the halo. Unfortunately neither of these models can be directly compared with the M33 results, and in any case the correct formulation is probably a synthesis of these two. The recent two-component galaxy models of Caimmi (1978*a*, *b*) offer

considerable promise in this regard, and a detailed attempt to model the observed gradient in the context of this theory is desirable.

VI. COMPARISON OF H II REGION/SNR GRADIENTS

Because of the well-known difficulties in obtaining electron temperatures from the [O III] λ4363 and [N II] λ5755 lines, the number of absolute abundance determinations in the literature on M33 is very sparse (Smith 1975; Peimbert and Torres-Peimbert 1977; Hawley and Grandi 1977; Edmunds and Pagel 1978). Consequently, investigators have been forced to use qualitative abundance indicators based on particular line ratios (Searle 1971; Benvenuti, D'Odorico, and Peimbert 1973; Jensen, Strom, and Strom 1976).

The H II regions selected for this study were chosen on the basis that (*a*) they were near an observed SNR and (*b*) the surface brightness of the H II region on a 48 inch Schmidt plate taken in the light of [S II] was similar to the SNRs. Inspection of the spectra (Table 2) so obtained shows that the second of these conditions ensured a strong selection to the low-excitation regions. As no temperature measurement is possible, we too are forced to use a qualitative abundance indicator, the [N II]/[S II] ratio. Benvenuti, D'Odorico, and Peimbert (1973) find evidence that these two emissions arise in the same volume; and since the temperature dependence of this ratio is negligible, then, to very good approximation (at the low-density limit of the [S II] ratio),

$$\frac{N(N^+)}{N(S^+)} = \frac{N(N)}{N(S)} = 4.95\,\frac{I(6548 + 84)}{I(6717 + 31)};$$

so in this sense it can be regarded as quantitative. Hawley and Grandi (1977) have discussed the limitations of this simple formula, showing in particular that the constant of proportionality between abundance and line ratio is a function of excitation.

The excitation level of the H II regions observed here ([O III] ≈ Hβ and strong [O II]) indicates a mean effective temperature of the exciting stars about 35000 K, or O8. For these, the correction factor is close to unity (0.86), so we believe that the above approximation to absolute abundance ratio is valid.

In Figure 6 we plot the N/S gradient given by the H II regions (*triangles*) with that given by the SNR (*circles*). The lines join H II regions with the nearest SNR. The agreement in both magnitude and shape is excellent, and within bounds determined by modeling errors in the two cases. Furthermore, the gradient between 3 and 5 kpc is very small [$d \log (N/S)/dr \approx -0.06$ kpc^{-1}], steepening sharply inside 3 kpc (-0.16 kpc^{-1}). (These are to be compared with the corresponding figures for the N/O gradient, 0.0 and -0.09, respectively.) On this basis, we are confident that the magnitude of the SNR derived abundance gradients is correct.

VII. NUCLEOSYNTHESIS OF NITROGEN

The nucleogenic status of nitrogen remains somewhat enigmatic. Talbot and Arnett (1973) emphasized

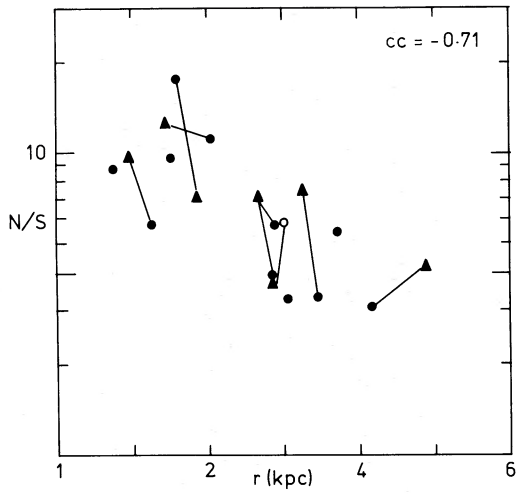

FIG. 6.—The comparison of enrichment theories and observed O abundance gradient. The compound power law (*solid line*) is based on the simple theory $n = 0$ in the inner regions and the Talbot and Arnett (1975) power law with index $n = 2$ in the outer regions ($r \gtrsim 2.5$ kpc). Metal enhanced star formation (MESF, Talbot and Arnett 1975) gives a reasonable fit for the stars (*) but far too high a gradient in the gas (G).

the difference between a primary and a secondary nucleosynthesis element. A primary element is with H or ^{4}He as its direct progenitor. This class includes C, O, Ne, Mg, Si, S, and Fe, and the ratio between the abundances of any two of these should be a constant provided production mechanisms are time-invariant. A secondary species, on the other hand, is one which is formed by subsequent processing in a star of the primary element. Such an element should increase its abundance as the square of the abundance of its primary progenitor. A good candidate for such an element was considered to be ^{14}N which is produced by the CNO cycle from the primary ^{12}C or (at higher temperature) from ^{16}O.

In Paper III (Dopita, Mathewson, and Ford 1977) the evidence from SNRs in our Galaxy and the Magellanic Clouds seemed to favor a secondary origin for ^{14}N, although this conclusion was heavily weighted by the anomalous superabundant SNR, Pup A.

The data from H II regions are equivocal. In our own Galaxy Peimbert, Torres-Peimbert, and Rayo (1978) give the ratio of N/H and O/H logarithmic abundance gradient as 1.77 whereas Hawley (1978) finds 1.66. On the other hand, Edmunds and Pagel (1978) find very little evidence for an N/O gradient in systems with lower N/O ratio than the Galaxy. Our results in M33 do not agree with this conclusion. Although in the outer regions there is indeed no N/O gradient, Figure 4 implies a ratio of 3.2 in the inner regions. This is probably an overestimate, because at high abundance the oxygen-to-nitrogen ratio is higher on Raymond's (1976, 1979) models than those used.

In Figure 7 we plot log N against log O using all the data including points from galaxies other than M33. The arrows connect values obtained with the Paper II

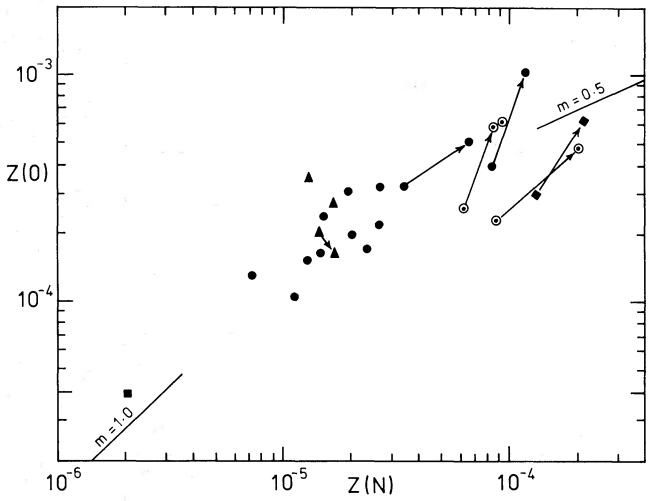

FIG. 7.—The correlation between N and O abundances determined from SNRs in the SMC (*filled squares*) (Dopita *et al.* 1977), the LMC (*filled triangles*), M33 (*filled circles*), the Galaxy (*partly filled circles*), and M31 (*filled diamonds*). Arrows connect Dopita (1976) models with Raymond (1976, 1979) models and show uncertainties due to modeling. This diagram seems to show that nitrogen, initially enriched as a primary element, becomes predominantly a secondary element for $Z(N) \gtrsim 2 \times 10^{-5}$.

models with the Raymond (1976, 1979) models, which represent extreme estimates according to Table 5. These models converge at the low-abundance end of the diagram, as can be seen by the LMC point representing N49. This diagram is similar to Figure 6 of Paper III, but the scatter has been very much reduced by better data.

The implication of Figure 7 is that *the sources of nitrogen enrichment change from primary to secondary as enrichment increases*, giving a change of slope from 1.0 to about 0.5 at $Z(N) = 2 \times 10^{-5}$, $Z(O) = 2.5 \times 10^{-4}$. We therefore require, as Edmunds and Pagel (1978), a primary source of nitrogen. The most likely candidates at present are the intermediate-mass stars (1–8 $M_\odot$) which can undergo surface enhancement of N and He by the dredging up of these elements during thermal pulses on the asymptotic giant branch (Iben and Truran 1978). Since some of these stars can form planetary nebulae, the theory has been tested for this class of objects with success (Kaler, Iben, and Becker 1979; Kaler 1979). Stars too massive to form planetaries will still return these products to the ISM in supernova explosions. Pup A (discussed above) may show this.

At high abundance, the total fraction of the mass formed into stars is greater and the mean age of the stars is greater. Hence, the second-generation stars generating nitrogen as a secondary element overwhelms the primary contributors, and the slope of Figure 7 changes.

We expect that observations of the SNR in NGC 300 (D'Odorico, Dopita, and Benvenuti 1979*a*) will provide an important check on the validity of these conclusions since the N/O ratio for this galaxy is very low (Edmunds and Pagel 1978).

As might be expected, the S/O ratio is constant within the limits of accuracy of the observations, proving that S, like O, is a primary element. From Figure 8, the S/O ratio is 1.5×10^{-2}; this is identical to the solar and solar system value (Pagel 1973).

VIII. CONCLUSIONS

To summarize the results presented here:

1. SNRs have been shown to be accurate tracers of the gas phase abundances in the interstellar medium.
2. We have confirmed the existence of large-scale radial abundance variations in the spiral arms of M33 in N, S, and O, and have been able, for the first time, to measure absolute abundance for many objects.
3. The gradient of the N/S abundance ratio for H II regions is the same as for SNRs.

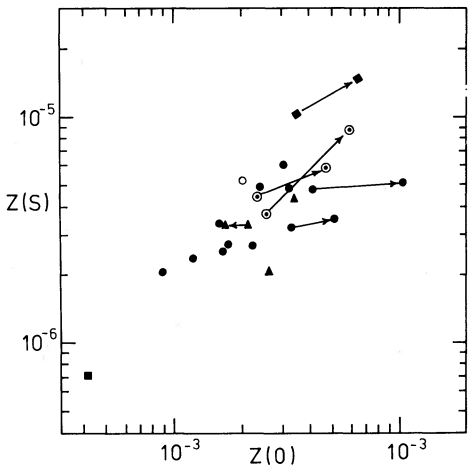

FIG. 8.—Same as Fig. 7 but for S and O. The Raymond models have been adjusted to give the same S abundance as the Dopita models for the LMC object N49 (see text). If O is purely primary, then this figure shows that S is also, and that $Z(S)/Z(O) = 1.5 \times 10^{-2}$.

4. A modification of the simple enrichment theory in which the star formation rate varies as a power of the density (Talbot and Arnett 1975) gives the best fit to the observations. Metal-enhanced star formation fails. However, no model is completely satisfactory, indicating that galactic enrichment theories are probably too simplistic.

5. Nitrogen has been shown to be enriched initially as a primary element, but at later times as a secondary element. Sulfur, like oxygen, is primary.

One of us (M. A. D.) wishes to thank Hale Observatories for the award of Guest Investigator privileges, for the generous amounts of telescope time allocated, and for the support of the technical staff at the telescope. He also wishes to thank A. Sandage, L. Searle, J. B. Oke, and D. Rubin for valuable discussions. S. D. acknowledges the support of a Visiting Fellowship to the ANU during which some of the work described in this paper was accomplished.

REFERENCES

Aller, L. 1942, *Ap. J.*, **95**, 52.
Benvenuti, P., D'Odorico, S., and Dopita, M. A. 1979, *Nature*, **277**, 99.
Benvenuti, P., D'Odorico, S., and Peimbert, M. 1973, *Astr. Ap.*, **28**, 447.
Boksenburg, A. 1972, Proc. ESO/CERN Conf. Auxiliary Instrumentation for Large Telescopes, Geneva, May 2–5, p. 295.
Boksenburg, A., and Burgess, D. E. 1973, *Proc. Symp. Astronomical Observation*, Vancouver, May 15–17, p. 21.
Bosma, A. 1978, doctoral thesis, University of Groningen.
Brocklehurst, M. 1971, *M.N.R.A.S.*, **153**, 471.
———. 1972, *M.N.R.A.S.*, **157**, 211.
Caimmi, R. 1978*a*, *Ap. Space Sci.*, **59**, 109.
———. 1978*b*, *Ap. Space Sci.*, **59**, 413.
Chevalier, R. A. 1975, *Ap. J.*, **200**, 698.
Chevalier, R. A., and Kirshner, R. P. 1978, *Ap. J.*, **219**, 931.
Collin-Souffrin, S., and Joly, M. 1976, *Astr. Ap.*, **53**, 213.
Comte, G. 1975, *Astr. Ap.*, **39**, 197.
Cowie, L. L. 1978, *Ap. J.*, **225**, 887.
Cox, D. P. 1972*a*, *Ap. J.*, **178**, 143.
———. 1972*b*, *Ap. J.*, **178**, 169.
Daltabuit, E., D'Odorico, S., and Sabbadin, F. 1976, *Astr. Ap.*, **52**, 93.
Danziger, I. J., Murdin, P. G., Clark, D. H., and D'Odorico, S. 1979, *M.N.R.A.S.*, **186**, 555.
de Vaucouleurs, G. 1959, *Ap. J.*, **130**, 728.
D'Odorico, S., Benvenuti, P., and Sabbadin, F. 1978, *Astr. Ap.*, **63**, 63.
D'Odorico, S., Dopita, M. A., and Benvenuti, P. 1979*a*, *Astr. Ap.*, in press.
———, 1979*b*, in preparation.
D'Odorico, S., and Sabbadin, F. 1976, *Astr. Ap.*, **50**, 315.
Dopita, M. A. 1974, *Astr. Ap.*, **32**, 121.
———. 1976, *Ap. J.*, **209**, 395 (Paper I).
———. 1977*a*, *Ap. J. Suppl.*, **33**, 437 (Paper II).
———. 1977*b*, *Astr. Ap.*, **56**, 303.
———. 1978, *Ap. J. Suppl.*, **37**, 117 (Paper IV).
———. 1979, *Ap. J. Suppl.*, **40**, 455 (Paper V).
Dopita, M. A., and Mathewson, D. S. 1979, *Ap. J.* (*Letters*), **231**, L147.
Dopita, M. A., Mathewson, D. S., and Ford, V. L. 1977, *Ap. J.*, **214**, 179 (Paper III).
Dufour, R. J. 1975, *Ap. J.*, **195**, 315.
Dufour, R. J., and Harlow, W. V. 1977, *Ap. J.*, **216**, 706.
Edmunds, M. G., and Pagel, B. E. J. 1978, *M.N.R.A.S.*, **185**, 77.
Gunn, J., Knapp, S., Oke, B., and Zimmerman, B. 1979, preprint.
Hawley, S. A. 1978, *Ap. J.*, **244**, 417.
Hawley, S. A., and Grandi, S. A. 1977, *Ap. J.*, **217**, 420.
Iben, I., Jr., and Truran, J. W. 1978, *Ap. J.*, **220**, 980.
Israel, F. P., and van der Kruit, P. C. 1974, *Astr. Ap.*, **32**, 363.
Iye, M., and Kodaira, K. 1975, *Pub. Astr. Soc. Japan*, **27**, 411.
Jensen, E. B., Strom, K. M., and Strom, S. E. 1976, *Ap. J.*, **209**, 748.
Kaler, J. B. 1979, *Ap. J.*, in press.
Kaler, J. B., Iben, I., Jr., and Becker, S. A. 1978, *Ap. J.* (*Letters*), in press.
Kamper, K., and van den Bergh, S. 1976, *Ap. J. Suppl.*, **32**, 351.
Kirshner, R. P., and Chevalier, R. A. 1978, *Astr. Ap.*, in press.
Kumar, C. K. 1976, *Pub. A.S.P.*, **88**, 323.
Larson, R. B. 1976, *M.N.R.A.S.*, **176**, 31.
Long, K. S., and Helfand, D. J. 1979, Columbia Astrophysics Laboratory preprint, No. 172.
Madore, B. F., van den Bergh, S., and Rogstad, D. H. 1974, *Ap. J.*, **191**, 317.
McKee, C. F., and Ostriker, J. P. 1977, *Ap. J.*, **218**, 715.
Mezger, P. G., Smith, L. F., and Churchwell, E. 1974, *Astr. Ap.*, **32**, 269.
Oke, J. B. 1974, *Ap. J. Suppl.*, **27**, 21.
Osterbrock, D. E., and Dufour, R. J. 1973, *Ap. J.*, **185**, 441.
Ostriker, J. B., and Thuan, T. X. 1975, *Ap. J.*, **202**, 353.
Pagel, B. E. J. 1973, in *Cosmochemistry*, ed. A. G. W. Cameron (Dordrecht: Reidel), p. 2.
———. 1978, General Lecture at 4th European Regional IAU Meeting in Astronomy, Uppsala, August 7–12.
Pagel, B. E. J., Edmunds, M. G., Fosbury, R. A. E., and Webster, B. L. 1978, *M.N.R.A.S.*, **184**, 569.
Parker, R. A. R. 1978, *Ap. J.*, **224**, 873.
Peimbert, M., and Torres-Peimbert, S. 1974, *Ap. J.*, **193**, 327.
———. 1977, *M.N.R.A.S.*, **179**, 217.
Peimbert, M., Torres-Peimbert, S., and Rayo, J. F. 1978, *Ap. J.*, **220**, 516.
Petrosian, V. 1973, in *IAU Symposium 52, Interstellar Dust and Related*, ed. J. M. Greenberg and H. C. van de Hulst (Dordrecht: Reidel), p. 445.
Pradhan, A. K. 1976, *M.N.R.A.S.*, **177**, 31.
Raymond, J. C. 1976, Ph.D. thesis, University of Wisconsin-Madison.
———. 1979, *Ap. J. Suppl.*, **39**, 1.
Rogstad, D. H., Wright, M. C. H., and Lockhart, I. A. 1976, *Ap. J.*, **204**, 703.
Rubin, V. C., Kumar, C. K., and Ford, W. K. 1972, *Ap. J.*, **177**, 31.
Sanduleak, N. 1969, *A.J.*, **74**, 47.
Sarazin, C. L. 1976, *Ap. J.*, **208**, 323.
Searle, L. 1971, *Ap. J.*, **168**, 327.
Searle, L., and Sargent, W. L. W. 1972, *Ap. J.*, **173**, 25.
Schmidt, M. 1959, *Ap. J.*, **129**, 243.
Shields, G. A., and Searle, L. 1978, *Ap. J.*, **222**, 821.
Shull, J. M. 1979, *Ap. J.*, **231**, 534.
Shull, J. M., and McKee, C. F. 1979, *Ap. J.*, **227**, 131.
Sivan, J. P. 1976, *Astr. Ap.*, **49**, 173.
Smith, J. E. 1975, *Ap. J.*, **199**, 591.
Talbot, R. J. 1974, *Ap. J.*, **190**, 604.
Talbot, R. J., Jr., and Arnett, W. D. 1973, *Ap. J.*, **186**, 51.
———. 1975, *Ap. J.*, **197**, 551.
Tinsley, B. M., and Larson, R. B. 1978, *Ap. J.*, **221**, 554.
van Genderen, A. M. 1969, *B.A.N. Suppl.*, **3**, 221.
Van Blerkom, D., and Arny, T. T. 1972, *M.N.R.A.S.*, **156**, 99.
Warner, P. J., Wright, M. C. H., and Baldwin, J. E. 1973, *M.N.R.A.S.*, **163**, 163.
Weaver, T. A., Zimmerman, G. B., and Woosley, S. E. 1978, *Ap. J.*, **225**, 1021.
Whitford, A. E. 1958, *A.J.*, **63**, 201.
Wray, J. D., and Corso, G. T. 1972, *Ap. J.*, **172**, 577.

M. A. DOPITA: Mount Stromlo and Siding Spring Observatories, Private Bag, Woden P.O. ACT 2606, Australia
SANDRO D'ODORICO and PIERO BENVENUTI: Osservatorio Astronomico di Asiago, Universita di Padova, Italy